Project: 1059
Project title: H2020 project BlueAction
Principal investigators: Dr. Daniela Matei, Dr. Elisa Manzini, Dr. Johann Jungclaus
Allocation period: 2020-01-01 to 2020-12-31

Achievements in 2020

In the reporting period, we have performed historical and hindcast simulations with the ocean eddy-resolving MPI-ESM1.2-ER model setup (Gutjahr et al., 2019, ER in the following), in coordination with the BMBF HiPred RACEII project. Our aim is to investigate potential improvements due to resolving eddies in interannual to decadal climate variability and in the prediction skill of the North Atlantic circulation and climate of the regions impacted by it (Europe, Nordic Seas, and Arctic). The ER setup has an eddy-resolving ocean component with a global resolution of 10 km and an atmospheric component with a resolution of 100 km (T127). We are comparing these eddy-resolving simulations with similar MPI-ESM1.2-HR experiments conducted within the BMBF MIKLIP II project (Marotzke et al., 2016) employing an eddy-permitting ocean resolution of 0.4° (~40km). Since both the radiative forcing (CMIP6) and the assimilation procedure are exactly identical, it allows us to isolate the effect of resolving eddies (and topographic features) in ER.

Besides performing three ensemble members of historical+ SSP2-4.5 scenario simulations with ER covering the period 1950 to 2100, we have conducted a set of multiyear hindcast simulations covering the period 1992 to 2014. To use the resources efficiently, the strategy so far was to spawn hindcasts every other year from an ER assimilation run conducted over the period 1992-2015. In the period under review, we have completed 12 hindcasts, each of which is now 3 years long. In the following, we summarize the results comparing these ER hindcasts with five members of the HR hindcasts of the MIKLIP prediction system.

1) Predictions of the SST in the subpolar gyre of the North Atlantic

The North Atlantic sea surface temperature (SST) has a strong influence on the climate of Europe (e.g. Årthun et al., 2017) and is one of the regions where models achieve a high predictability (e.g. Matei et al., 2012; Müller et al., 2012; Marotzke et al., 2016). Beside other factors, such as the assimilation technique or the type of assimilation data, the model resolution was found to affect the predictive skill as well (Prodhomme et al., 2016). Prodhomme et al. (2016) increased the ocean resolution from 1° to 0.25° and found improvements of model biases and also of the prediction skill. Here we go beyond and analyse improvements of prediction skill in the MPI-ESM1.2 prediction system resulting from an ocean eddy-resolving (0.1°) component. To assess the performance of the MPI-ESM1.2-ER prediction system, we have conducted 12 hindcast simulations that are 3-years long each, as outlined above. These hindcasts used the same assimilation technique and data as the hindcasts performed with MPI-ESM1.2-HR within the MIKLIP project (Pohlmann et al., 2019) with all three climate system components (ocean, atmosphere, sea ice) initialised from observations.

Figure 1 depicts the time series of annual mean SST averaged over the North Atlantic subpolar gyre (60°E-15°W and 50°- 65°N). The SST time series from the observations show both the distinct abrupt strong warming shift of 1995 and the cooling trend in the 2010s that culminated with the record cold blob conditions of 2015 (Duchez et al., 2016). Comparing the lead year 1 (first year after initialisation) time series of the hindcasts from ER with HR, there is a clear reduction in the systematic model bias by using an eddy-resolving ocean component in ER (Fig. 1a). All HR hindcasts are approximately 1°C too warm, but the ER hindcast is very close to the observations. This improvement of the SST bias in ER was also reported by Gutjahr et al. (2019) for a 1950 control simulation with ER. Although all simulations are able to reforecast the warming in the mid 1990s and the cooling from about 2010 onwards, the warming is less in the first half of the 1990s than observed one.

After removing the model systematic bias, the reforecasted SST anomalies agree well with the observations to a first order (Fig.1b), with a Pearson correlation coefficient of about 0.4. However, again we note that the warm anomaly in the mid1990s is slightly less than in the observations, but consistent in all hindcasts, whereas there is much more uncertainty (spread of the hindcasts) for the sharp cold blob anomaly in 2015. Summarizing common statistical measures for comparing time series in a Taylor diagram (Fig. 1c), we find that one ensemble member ER hindcasts cannot be distinguished with respect to anomalies, but reducing the SST bias in the North Atlantic probably will have implications for other quantities than SST, such as storm tracks or blocking events over Europe.

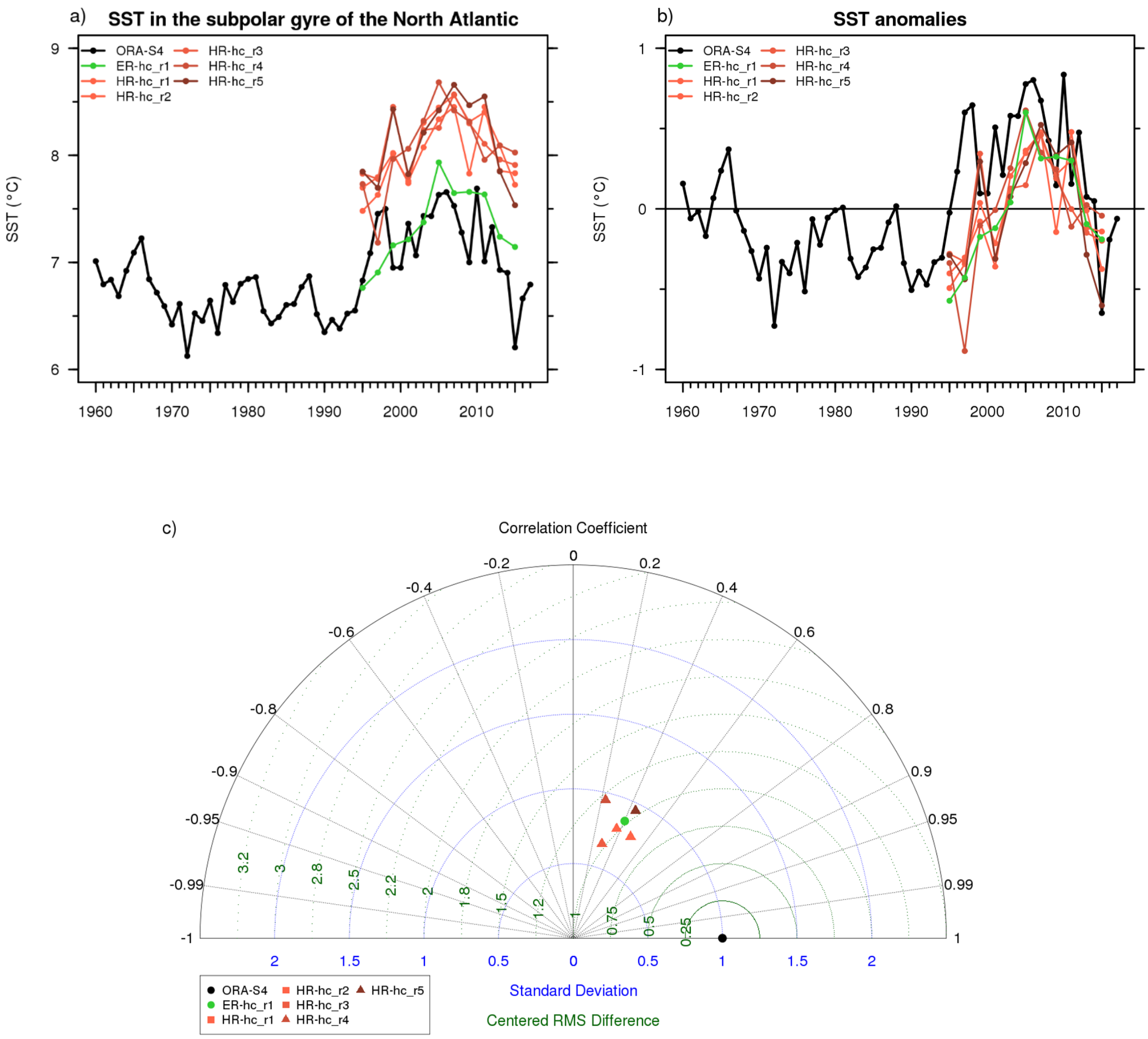

Figure 1: *Time series of (a) absolute sea-surface temperature (SST) and (b) SST anomalies in the North Atlantic subpolar gyre (60° to 15°W and 50° to 65°N) over the period 1960-2017 from observations (ORA-S4) and MPI-ESM1.2 hindcasts (1995-2015) with ER and HR setups. Subfigure (c) shows a Taylor diagram of the SST anomalies from (b).*

2) Case study: North Atlantic record "Cold Blob" and European heat waves in the summer of 2015

Because of this large uncertainty of the hindcasts in 2015 due to the chaotic nature of the atmosphere and its particular sensitivity to the initial values, we have made a more detailed comparison for the development of the two strong anomalies that coexisted in 2015: the record "Cold Blob" in the North Atlantic and the summer heat-waves over Europe. From Fig.1 we conclude that both prediction systems are capable of reproducing a cold anomaly over the North Atlantic in 2015, but the strength of the anomaly is subject to a great uncertainty. Only one of the five HR members is able to reforecast the observed magnitude of the cold anomaly (Fig.1b). The reason why the spread of the hindcasts increase in 2015 is that the models first need to simulate a persistent strong NAO+ phase during the winter and spring of 2015, resulting in a western flow that constantly removes heat from the ocean to produce the "Cold Blob", and second the right timing of blocking events over Europe by a high pressure ridge that lead to the heat waves in the summer of 2015. Such complex conditions require a large ensemble of hindcasts to increase the signal-to-noise ratio. Understanding the reasons behind this challenge in successfully forecasting the North Atlantic "Cold Blob" event and associated impacts over European continent are currently subject to sustain efforts in the decadal prediction research community (e.g. Maroon et al., 2020). Particularly, the H2020 Blue-Action project has identified this impact-relevant extreme climate event as a test-bed for future development of multi-year-to-decadal prediction systems.

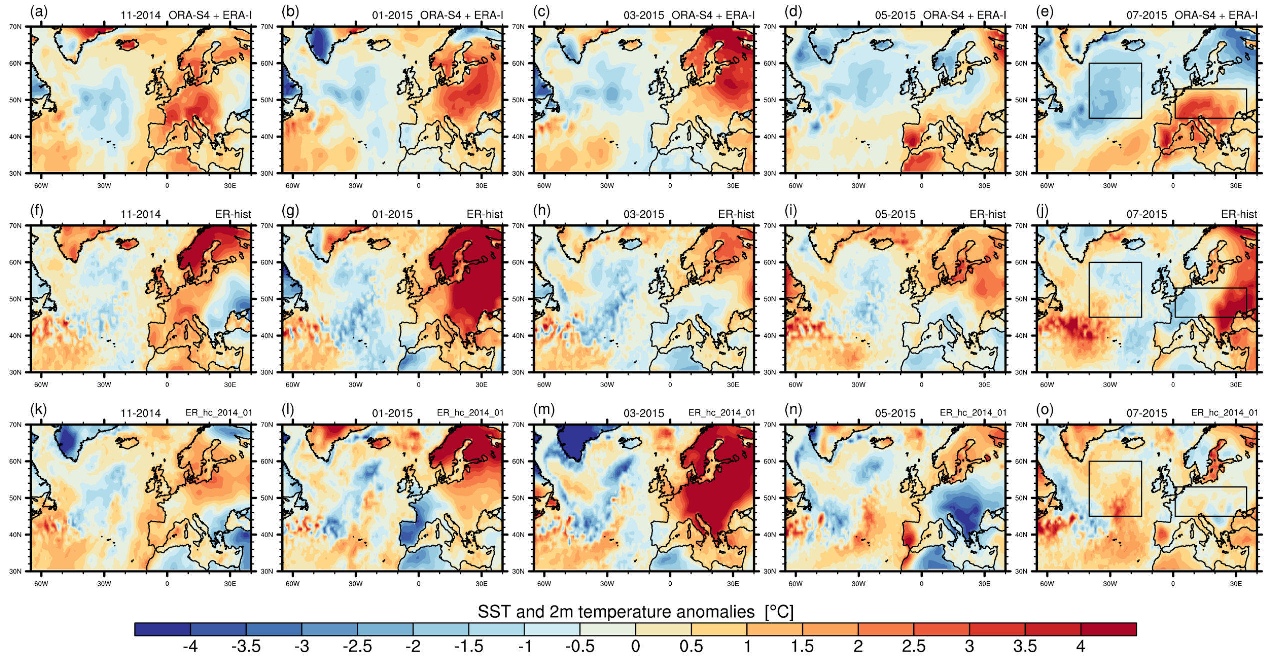

Figure 2: *Monthly mean anomalies of sea surface temperature (SST) and 2m temperature from November 2014 to July 2015 relative to the mean 1981-2010. Top row: a composite of SST from ORA-S4 and 2m temperature from ERA-Interim. Middle row: first ensemble member of the ER historical simulations (ER-hist). Bottom row: First ensemble member of the ER hindcasts initialised on 1st November 2014. The black boxes in the last column illustrate the center of the SST cold anomaly in the North Atlantic and of the heat wave over central Europe.*

Figure 2 shows a composite of SST (over ocean) and 2m temperature (over land) and how it changes from November 2014 to July 2015. Already beginning in November there is a cold anomaly ("blob") observed (Fig. 2a) that is about -2°C colder than on average and persists until July 2015 and thereafter. This cold blob developed due to a persistent strong wind forcing in a NAO+ phase that was maintained for about 6 months and caused an anomalously large heat loss to the atmosphere. Figure 3 (top row) shows a strong meridional gradient of the 850hPa geopotential over the North Atlantic that caused a strong western flow, which removed a large amount of heat from the ocean. This almost zonal flow remained until approximately March, where it already became unstable and was blocked by a high pressure system that moved over Europe. This high pressure ridge then caused very weak wind conditions and shuffled warm air masses to central Europe, which resulted in a heat wave (Fig. 2e) that was within the top 10 of the last 65 years (Russo et al., 2015).

So far, we compared one member of the historical simulations with ER (ER-hist) and one member of the ER hindcasts that were initialised on 1st November 2014 (ER_hc_2014_01). We find that the selected historical simulation coincides to some degree by chance with the observations for this period, while the other historical ensemble members do not. Both the historical and the hindcasts with ER reproduce the cold anomaly in the North Atlantic, although less pronounced than observed, and maintain a "Cold Blob" until March 2015, before the anomaly vanishes. Without simulating a correct strong cold anomaly the meridional pressure gradient weakens to early so that the high pressure ridge moves northward either too early (Fig. 2n) or has a wrong location (Fig. 2j).

Predicting such extreme coupled climate phenomena over the North Atlantic-European region has proved to be very challenging for state-of-art prediction systems (Maroon et al, 2020). However, we could demonstrate that our prediction system is able to reproduce the observed anomalies but in years where it is absolutely necessary to forecast the atmosphere conditions too, it will require a large ensemble of hindcasts (of the order of 10 or more). We could also demonstrate that using an eddy-resolving ocean (0.1°) improves considerably the model systematic bias over the North Atlantic subpolar gyre. Based on these promising results, we plan to investigate other phenomena such as storm frequencies or blocking events over Europe, but also forecasting the Arctic sea ice. However, in order to attain statistical robustness we will have to produce more ensemble members with the ER model.

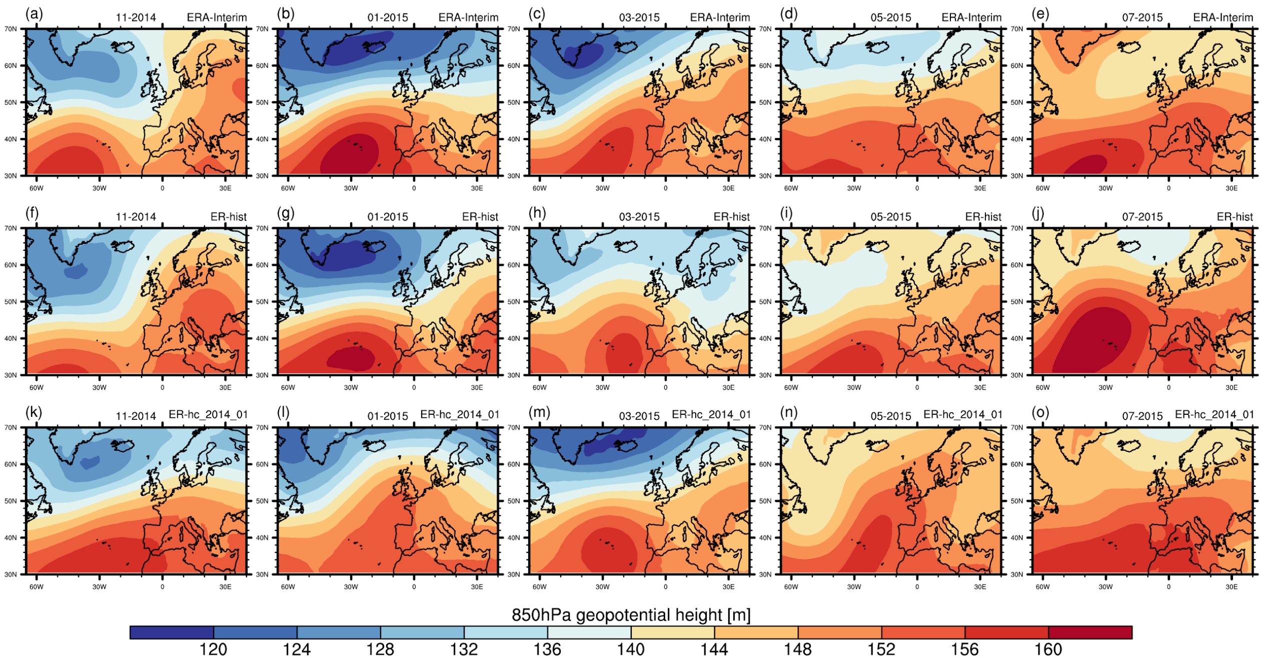

Figure 3: *Monthly means of the 850 hPa geopotential height from November 2014 to July 2015. Top row: from reanalysis ERA-Interim. Middle row: first ensemble member of the ER historical simulations (ER-hist). Bottom row: First ensemble member of the ER hindcasts initialised on 1st November 2014.*

3) Artic sea ice loss and mid-latitude climate variability

The role of Arctic sea ice loss in the recent Eurasian winter cooling remains debated due to contradictory results from observations and models. Experiments with the atmospheric component of the MPI-ESM model, carried out under this project, are part of a unique large multi-atmospheric-model ensemble experiments, which has proven key in our understanding of the of Artic – mid latitude climate linkages (Ghosh et al 2020). Specifically, we investigated two sets of experiments. In the first experiment (hereafter ALL), the atmospheric model is forced with the observed estimate of daily sea surface temperature (SST) and Arctic sea ice concentration (SIC), from 1980 to 2014. The second experiment (hereafter SICclim) has the same boundary conditions except for the Arctic (SIC), which is prescribed by its daily climatology. With the MPI-ESM atmospheric component (ECHAM6.3) of the MPI-ESM, we contributed an ensemble of 10 members to each experiment set. The multi-atmospheric-model ensemble comprises in total of 145 members, for each experiment, from eight different atmospheric models. Our analysis focuses on the Northern hemisphere winter, when Artic sea ice impacts can be large. To this end, in the following results are based on seasonal means from December to February (DJF).

We find that the second mode of Eurasian surface air temperature (SAT) DJF variability, the Warm Arctic-Cold Eurasia (WACE) pattern, exhibits a consistent positive trend in response to the observed Arctic SIC loss (ALL ensemble, Fig. 4 right, grey ensemble and red lines). Instead, there is no trend in the WACE time series when the prescribed Arctic SIC remains climatological (not shown). Our finding from the comparison of the multi-model ensemble with and without SIC variability and trends therefore provide support for the attribution of the observed trend in the DJF WACE pattern to Arctic sea ice loss (also shown in Fig. 4 right, estimated by ERA Interim reanalysis (ERAI) for the period 1980 to 2014, black, and to 2019, orange lines). In Fig. 4 (right) we show in addition that the WACE pattern has continued and strengthened up to winter 2019 and that there is a close relationship with the observed WACE and BS SIC trend and variability. These results bring consensus between the observational and modeling results and displays an important role of Arctic SIC loss for the Eurasian winter temperature variability and trends.

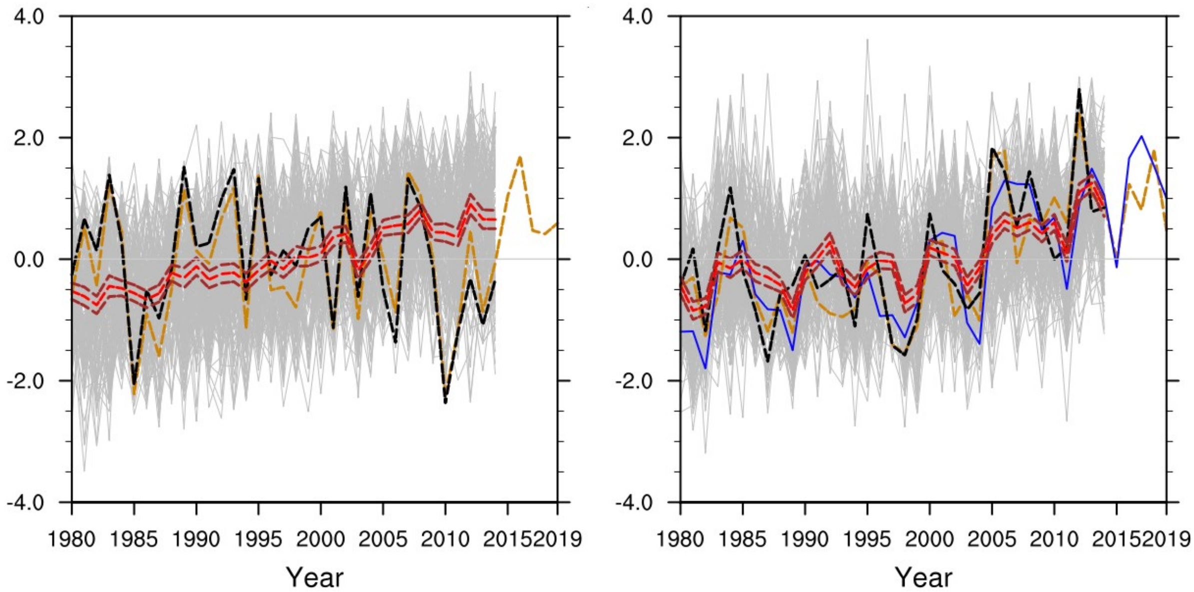

Figure 4. *Northern Hemisphere winter dominant SAT modes of variability. The modes are extracted by EOF analysis over the Eurasian region (20°-90°N, 0°-180°E). Shown are the normalized principal component time series, PC1 at left and PC2 (the WACE pattern) at right. The black and orange lines are from ERAI data for the period 1980 – 2014 and 1980- 2019 respectively. The normalized PC timeseries for each of the 145 ensemble members of the ALL experiment are shown in grey. The red lines are the ensemble mean of the modelled PC timeseries, showing the forced response, and the brown lines are the 95% confidence intervals of the ensemble means. The additional blue curve (right panel) is the normalized sign reversed timeseries of the winter area averaged (74N-80N, 20E-68E) Barents Sea SIC. From Ghosh et al (2020).*

However, the consensus between the observational and modeling results does not extend to the first mode (PC1) of Eurasian SAT variability (Fig. 4 left). Whereas there is no trend in the observed PC1 timeseries estimated by ERAI (Fig. 4 left, black and orange lines), a clear trend emerges from the modelled PC1 timeseries Fig. 4 left, grey ensemble and red lines).

PC1 of Eurasian SAT in observations is related to the first dynamical mode of sea leave pressure variability, the Arctic Oscillation (AO), a see-saw pattern of sea leave pressure variability in NH (20°N-90°N, 180°W-180°E). The correlation between PC1 and AO is 0.85 (Fig. 5 left, vertical back line). The strength of this relationship is lowered in our experiments, especially when the Arctic SIC forcing is considered (Fig. 5 left, brown bars). The peak of the correlation from the ALL experiment is indeed between 0.6 and 0.7. Given the crucial role of PC1 in the overall Eurasian SAT trend, the disassociation of PC1 and AO in the models calls for further investigation, to be addressed in a follow up work. So far, preliminary investigations suggest that the PC1-AO disconnect is related to a too strong thermal response to BS SIC loss and/or a lack of trend in AO related dynamics in the models. The latter is shown in Fig. 5 right, in terms of 10 hPa zonal mean zonal wind trend, given the known relationship between sea leave pressure variability and the stratosphere. Stratosphere-troposphere coupling could indeed be crucial for both the AO variability and the strength of the link between Arctic SIC loss and stratospheric polar vortex slowdown, which in turn could reduce the thermal response in PC1. Other sources of inconsistencies could stem from the misrepresentation of sea ice physics, ocean-atmosphere teleconnections.

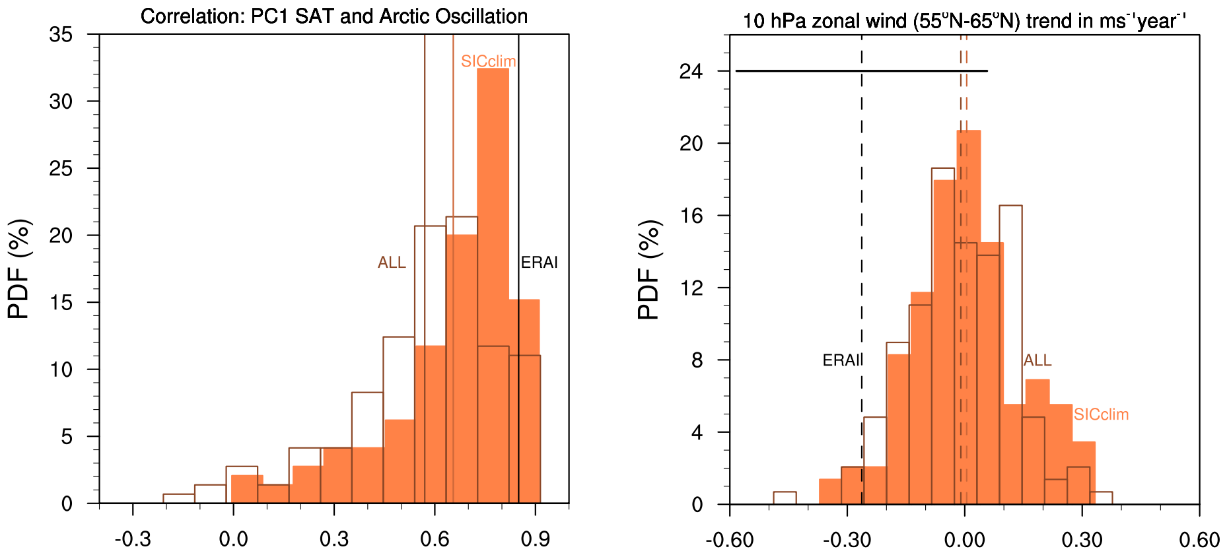

Figure 5. *(left) Correlations between the PC1 and AO time series. The pdf of the correlation from the ALL experiment (brown bars) and the SICclim experiment (sienna filled bars). The brown and sienna vertical lines are the corresponding ensemble means. The black line is the correlation in ERAI. (right) Trends in 10 hPa zonal mean zonal wind averaged between 55°N-65°N. The pdf of the trends from the ALL experiment (brown bars) and the SICclim experiment (sienna filled bars). Brown and sienna vertical dashed lines (not significant at 5% level) show the corresponding ensemble means. The black vertical dashed line shows the same in ERAI and the associated black horizontal line shows the 95% confidence interval of that trend. From Ghosh et al (2020).*

References

Århun, M., Eldevik, T., Viste, E., Drange, H., Furevik, T., Johnson, H.L., Keenlyside, N. S., 2017: Skillful prediction of northern climate provided by the ocean. Nature Communications, 8, 15875, doi: 10.1038/ncomms15875.

Duchez, A. et al. (2016), Drivers of exceptionally cold North Atlantic Ocean temperatures and their link to the 2015 European heat wave. Environ. Res. Lett., 11, 074404, doi: 10.1088/1748-9326/11/07/074004.

Ghosh, R., E. Manzini, Y. Gao, G. Gastineau, A. Cherchi, C. Frankignoul, Y.-C. Liang, Y.-O. Kwon, L. Suo, J. V. Mecking, T. Tian, Y. Zhang, and D. Matei (2020) A clear role of Arctic sea ice loss for the winter Warm Arctic Cold Eurasia trend, under review by *Nature Communication*.

Gutjahr, O., Putrasahan, D. A., Lohmann, K., von Storch, J.-S., Jungclaus, J. H., Brüggemann, N., Haak, H., Stössel, A., 2019: Max Planck Institute Earth System Model (MPI-ESM1.2) for High-Resolution Model Intercomparison Project (HighResMIP). *Geoscientific Model Development*, 12, 3241-3281, doi: 10.5194/gmd-12-3241-2019.

Matei, D., H. Pohlmann, J. Jungclaus, W. Müller, H. Haak, J. Marotzke, 2012: Two tales of initializing decadal climate prediction experiments with the ECHAM5/MPI-OM model. *J. Climate*, 25, 8502-8523.

Maroon, E., S. Yeager, G. Danabasoglou, N. Rosenbloom, 2020: Was the 2015 North Atlantic subpolar cold anomaly predictable? , submitted to *J. Climate*.

Marotzke, J., Müller, W. A., Vamborg, F. S. E., Becker, P., Cubasch, U., Feldmann, H., Kaspar, F., Kottmeier, C., Marini, C., Polkova, I., and others: MIKLIP - a national research project on decadal climate prediction. Bull. Amer. Meteor. Soc., 97, 2379-2394, doi: 10.1175/BAMS-D-15-00184-1.

Müller, W. A., Baehr, J., Haak, H., Jungclaus, J. H., Kröger, D., Matei, D., Notz, D., Pohlmann, H., von Storch, J.-S., Marotzke, J., 2012: Forecast skill of multi-year seasonal means in the decadal prediction system of the Max Planck Institute for Meteorology. Geophys. Res. Lett., 39, L22707, doi: 10.1029/2012GL953326.

Pohlmann, H., Müller, W.A., Bittner, M., Hettrich, S., Modali, K., Pankatz, K., Marotzke, J., 2019: Realistic quasi-biennial oscillation variability in historical and decadal hindcast simulations using CMIP6 forcing. Geophys. Res. Lett., 46, 14118-14125, doi: 10.1029/2019GL084878.

Prodhomme, C., Batté, L., Massonnet, F., Davini, P., Bellprat, O., Guemas, V., Doblas-Reyes, F.J., 2016: Benefits of increasing the model resolution for the seasonal forecast quality in EC-EARTH. J. Climate, 29, 9141-9162, doi: 10.1175/JCLI-D-16-0117.1.

Russo et al. (2015), Top ten European heatwaves since 1950 and their occurrence in the future. Environ. Res. Lett., 10, 123003, doi: 10.1088/1748-9326/10/12/124003.